Applied Energy 362 (2024) 122954

Contents lists available at ScienceDirect

Applied Energy

journal homepage: www.elsevier.com/locate/apenergy

Techno-economic assessment of future vanadium flow batteries based on real device/market parameters

Nicola Poli [a,b], Cinzia Bonaldo [c], Michele Moretto [b,d], Massimo Guarnieri [a,b,*]

[a] Department of Industrial Engineering, University of Padua, Padova, Italy
[b] Interdepartmental Centre Giorgio Levi Cases for Energy Economics and Technology, University of Padua, Padova, Italy
[c] RSE S.p.A., Ricerca Sistema Energetico, Milano, Italy
[d] Department of Economic and Management, University of Padua, Padova, Italy

HIGHLIGHTS

- A techno-economic model for vanadium redox flow battery is presented.
- The method uses experimental data from a kW-kWh-class pilot plant.
- A market analysis is developed to determine economic parameters.
- Capital cost and profitability of different battery sizes are assessed.
- The results of prudential and perspective analyses are presented.

GRAPHICAL ABSTRACT

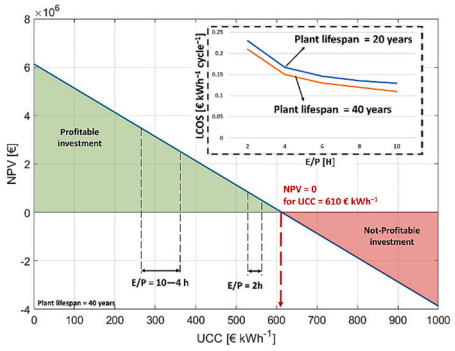

ARTICLE INFO

Keywords:
Energy storage system
Renewable energy
Vanadium flow batteries
Flow batteries
Profitability analysis
Economic model
Key performance indicator

ABSTRACT

This paper presents a techno-economic model based on experimental and market data able to evaluate the profitability of vanadium flow batteries, which are emerging as a promising technology for specific stationary energy services. Models like this are very informative on the present and perspective competitivity of industrial flow batteries in operating specific services, but they have not yet been developed to an accurate grade. This model uses technical parameters which are taken from large-area multi-cell stacks, rather than from small single cell experiments, to better characterize the behavior of real industrial reactors, and from real financial market and economic patterns of some major manufacturers. The model yields economic performance indicators as the capital cost, the operative cost, the levelized cost of storage and the net present value. A prudential present-state and a perspective analysis are elaborated to show where the economic indicators are heading, and which parameters affect more the investment profitability, thus tracking a possible roadmap for system optimization. Perspective estimations indicate that technological and market evolutions are heading to much more competitive systems, with capital costs down to 260 € kWh^{-1} at a energy/power duration of 10 h, to be compared with a break-even point in the net present value of 400 € kWh^{-1}, which suggests that flow batteries may play a major role in some expanding markets, notably the long duration energy storage.

* Corresponding author at: Department of Industrial Engineering, University of Padua, Padova, Italy.
E-mail addresses: massimo.guarnieri@unipd.it, massimo.guarnieri@dii.unipd.it (M. Guarnieri).

https://doi.org/10.1016/j.apenergy.2024.122954
Received 10 June 2022; Received in revised form 2 February 2024; Accepted 1 March 2024

Nomenclature

Acronyms and symbols

A	Area [m^2]
ac/dc	alternating current / direct current
ASR	Area specific resistance [Ω cm^2]
BMS	Battery management system
BOP	Balance of plant
c	Specific cost / price [€ (specific unit)$^{-1}$]
C	Cost [€]
CAPEX	Capital expenditure [€]
CAPM	Capital asset pricing model
DOD	Depth of discharge [%]
E	Energy [Wh]
E_0'	Corrected cell standard potential [V]
EES	Electrochemical energy storage
EESS	Electrochemical energy storage system
EOL	End of life
ES	Energy storage
ESS	Energy storage system
f	Material factor
F	Faraday's constant = 96,485 [C mol^{-1}]
FB	Flow Battery
FR	Fade rate [% $month^{-1}$]
j	Current density [A cm^{-2}]
KPI	Key performance indicator
LCOS	Levelized Cost of Storage [€ kWh^{-1} $cycle^{-1}$]
LDES	Long Duration Energy Storage
M	Molar concentration [mol m^{-3}]
MRP	Market risk premium
n	Number of events per year
N	Number of units (cells, stacks, …) or events
NPV	Net Present Value [€]
OCV	Open circuit voltage [V]
OPEX	Operational expenditure [€]
p	Price
P	Power [W]
PCS	Power conditioning system
PUN	National single price (Italian)
r	Discount rate [%]
R	Revenue [€]
$\overline{R}$	Gas constant = 8.314 [J K^{-1} mol^{-1}]
r_f	Risk-free interest rate
RTE	Round-Trip Efficiency [%]
SOC	State of charge [%]
t	Time [year] or [h] or [min] or [s]
U	Cell voltage [V]
UCC	Unit capital cost (*CAPEX* per unit energy) [€ kWh^{-1}]
UOC	Unit operating cost (*OPEX* per unit energy) [€ kWh^{-1}]
V	Volume [m^3]
VFB	Vanadium, Flow Battery
VRES	Variable renewable energy source
z	Number of electrons per reaction
α	Cost extrapolation parameter
β	Investment systematic risk
η	Efficiency [%]

Subscripts

a	Equipment with the known/unknown cost – Eq. (14)
ass	Assembly
b	Equipment with known cost – Eq. (14)
bp	Bipolar plate
c	Cell
cc	Current collector
cr	Crossover
e	Electricity
E	Energy
ec	Electric circuitry
ed	electrode
el	Electrolyte
ff	Flow-frame
g	Gasket
h	hydraulic
i	Year index
loss	Loss
m	Membrane
max	Maximum
min	Minimum
mix	Mixing process
ox	Oxidative
P	Power
pcs	Power condition system
reg	Regenerating process
RT	Round-trip
S	Stack
sh	Stack head
t	Tank
V	Vanadium
y	Years of plant lifespan

1. Introduction

1.1. Present scenario of energy storage

Future decarbonized grids will need Energy Storage (*ES*) to support non-dispatchable Variables Renewable Energy Sources (*VRESs*), notably photovoltaics and wind, in equating the daily load demand dynamics. In fact, while the world's *VRES* capacity reached 3064 GW with a production of 7456 TWh in 2021, *ES* global capacity grew to 172 GW and 1.62 TWh [1,2]. *ES* Systems (*ESSs*) which totalize these figures present power capacity up to few GW and storage capacity up to few tens of GWh. Growing together in the next decades, *VRESs* and *ESSs* are expected to meet the target of phasing out fossil sources by 2050. In order to complement *VRESs* in decarbonized grids, *ESSs* will provide both fast and long (i.e. Long Duration Energy Storage – *LDES*) services [3], e.g. frequency regulation [4], peak shaving [5], load leveling [1], energy arbitrage [2], seasonal storage [3], and even more [6,7]. Primary reserve services via *ESS* is also increasingly important for Transmission System Operators (TSOs), as attested by the €348 M Netzbooster Project in Germany and the €80 M RINGO Project in France [8,9]. The Italian PNIEC (acronym for *national integrated plan for energy and climate*) includes among its targets the development of a storage capacity of 6 GW by 2030 (including pumped hydro energy storage) [10] and the Italian TSO Terna allotted 250 MW of *ES* in a December 2020 auction for a Fast Reserve project focused on batteries for dispatching services [11].

1.2. Electrochemical energy storage systems and flow batteries

Electrochemical *ES* (*EES*) is particularly versatile and several investigations indicate it as the solution of choice for providing different storage services, because their modularity and scalability allow power ratings from few kilowatts to many megawatts in a wide range of discharge times, up to some hours. In addition, they are capable of fast responses, in the order of milliseconds, and are exempt from

geomorphological constraints so that they present advantages hardly available in other storage technologies [12].

The main issue to a widespread diffusion of large stationary *EES* Systems (*EESSs* comes from their high costs, limited number of charging/discharging cycles, safety issues, low recyclability, and sustainability of raw materials [14]. Some key performance indicators (*KPIs*) of the main *EES* technologies taken from the literature are compared in Table 1. Lithium-ion batteries present the lowest *UCC* and *LCOS*. This fact justifies their present market success. Nevertheless, flow batteries (*FBs,* also redox flow batteries – *RFBs*) present a number of features which make them particularly promising among other electrochemical storage technologies [15,16]. The all-vanadium *FB* (*VFB*) is the most developed among them. Its advantages over other batteries are [15]: 1) independent sizing of power and energy; 2) long cycling life (even >20,000 cycles are claimed); 3) high operation safety with no fire or explosion risk; 4) complete electrolyte recyclability [17,18]. *VFBs* are already marketed, with 27 producers worldwide and the global vanadium organization VANITEC in listing the plants installed globally accounts for a total power capacity exceeding 500 MW and energy capacity above 1.5 GWh [19]. However, some challenges remain to be addressed to take *VFBs* to a high competitivity, notably low energy density and high investment cost [20].

1.3. VFB technoeconomic analyses

The US Department of Energy (*DOE*) fixed a capital cost target for *ES* of 100–150 \$ kWh^{-1} (94–140 € kWh^{-1}) and a Levelized Cost of Storage (*LCOS*) of 0.05 € kWh^{-1} $cycles^{-1}$ [21]. The latter is a more complete, though somewhat neglected, economic indicator as it is detailed further on. In this framework, several recent economic analyses indicate for *VFBs* a capital cost in the range of 300–800 € kWh^{-1} (or even less) [22] and a *LCOS* ranging as 0.1–0.5 € kWh^{-1} $cycles^{-1}$ [23,24]. Such wide ranges are due to the different sizes in terms of energy to power ratio *E/P*, and also to the different assumptions considered. In fact, some analyses take into account the major battery components only, notably the electrolytes with tanks and electrochemical reactors (i.e. the stacks) [25,26], others take into account the whole system, including the balance of plant (*BOL* i.e. every supporting component and auxiliary subsystems such as piping, pumps, instrumentation, power conditioning system, and battery management system, needed for a complete safe battery operation) [22,27]. The rated power of the analyzed systems ranges between 2 and 50,000 kW, with a most commonly found value of 1000 kW. The *E/P* ratio is mostly between 4 and 12 h, with a wide range of 0.25–150 h considered in a recent study [23]. The depth of discharge is assumed as 80% in the majority of studies, nevertheless, values of up to 100% are sometimes considered [23]. The current density is typically 40–50 mA cm^{-2} but values up to 100 mA cm^{-2} are considered [23]. Cells with rectangular active area between 0.1 and 1.0 m^2 are typically assumed, while the concentration of vanadium in the electrolyte ranges as 1.4–1.8 M with upper limits up to 2.0–2.5 M as prospective figs. [23]. In this wide scenario, only few studies include operational and maintenance costs, although these expenditures constitute important items of a comprehensive economic analysis [28–30]. Moreover, even though some techno-economic assessments are very detailed, the majority of them, to the best of our knowledge, use data from simple laboratory experiments which use single-cell or short small stacks of few cells. In addition, economic parameters such as the discount rate and the electricity price, whose values depends on financial conditions, require a specific methodology for their calculation, which, in most studies, is not considered [23,31–33].

This work presents a techno-economic assessment of industrial *VFB* systems that considers a detail physical model in which the variability of physical parameters is duly taken into account, being deduced by the experimental data of a test facility provided with a large-area multi-cell stack, suitable for industrial uses. In this approach, all components affecting the capital and operative costs could be considered accurately and side phenomena causing capacity losses and their cost impact could be accounted as well. Parametric updated of the physical model features allowed adaptation to the recent state-of-the-art systems, which were carried out in the aim of model sensibility. In the same spirit, the battery capacity losses were also considered. Discount rate and electricity price were calculated based on real market data. The paper is structured as follows: the economic model is presented in Section 2, starting from a brief description of the *VFB* facility from which experimental parameters were extracted; economic and technical parameters adopted for the analysis are discussed in Section 3; the prudential and perspective *KPIs* of the analysis are presented in Section 4; the conclusions are drawn in Section 5.

2. Model

2.1. LCOS and NPV

Two economic *KPIs* which assess the competitiveness of an energy storage system are: the Levelized Cost Of Storage (*LCOS*) and the Net Present Value (*NPV*). The former is the ratio between the discounted total costs of the battery and the discounted energy stored over a project lifespan [13,28]:

$$LCOS = \frac{CAPEX + \sum_{i=0}^{y} \frac{OPEX_i}{(1+r)^i} + \sum_{i=0}^{y} \frac{E_i\, c_e}{(1+r)^i} + \frac{C_{EOL}}{(1+r)^{y+1}}}{\sum_{i=0}^{y} \frac{E_i\, \eta_{RT}}{(1+r)^i}} \left[€\ kWh^{-1} cycle^{-1}\right] \quad (1)$$

where *CAPEX* is the capital cost, *OPEX* is the yearly operative and maintenance costs, E_i is the charging battery energy per year, c_e is the purchase price of the energy, r is the yearly discount rate and η_{RT} is the round-trip efficiency (*RTE*). $E_i c_e$ represents the yearly charging cost. The operative costs, the charging cost and the stored energy are tracked yearly, vs the year index $i = [1, y]$. The End-Of-Life (*EOL*) cost C_{EOL} occurs once the useful life of the battery is over.

The *NPV* is the difference between the discounted cash flows obtained during the lifespan and the investment costs of the technology [28]:

Table 1
Main key performance indicators (*KPIs*) of some battery technologies for stationary applications [13]. Both these reports assume zero end of life costs for all compared technologies. H_2-EL-FC = hydrogen-electrolyzer-fuel cell; Pb-A = lead-acid; Na-Ni-Cl = Zebra-Sonick; Na-S = Sodium-Sulfur; *VFB* = all-vanadium flow battery; Li-ion = lithium ion.

KPI	H_2-EL-FC	Pb-A	Na-Ni-Cl	Na-S	VFB	Li-ion
Lifecycle [n. of cycles]	500	800–1000	4500	4500	20,000	5000
Energy density [Wh kg^{-1}]	800–1000	25–50	95–120	150	25–30	100–200
Recyclability	high	high	medium	medium	high	low
Safety	Low	Low	Low	Low	High	Low
Self-discharge	Low	Low	High	High	Low-High	High
RTE [%]	20	75	90	90	70–80	90
UCC [€ kWh^{-1}]	1000–2000	600–800	500–600	400–600	300–800	200–300
LCOS [€ kWh^{-1} $cycle^{-1}$]	0.6–1.2	0.5–0.8	0.3–0.5	0.2–0.4	0.1–0.5	0.1–0.3

$$NPV = -CAPEX + \sum_{i=0}^{y} \frac{E_i(p_e\eta_{RT} - c_e) - OPEX_i}{(1+r)^i} \ [€] \quad (2)$$

where p_e is the sales price of electricity. The factor $(p_e - c_e)$ represents the net revenues, i.e., the revenues deriving from selling – and consequently delivering in the grid – electricity net of the costs of electricity taken from the grid and stored. The *NPV* indicates if the investment will be profitable or not. If $NPV < 0$ it is not worth to invest in the project, on the contrary if $NPV > 0$ revenues result higher than costs so it is worth to invest in the project.

The two indicators of Eqs. (1) and (2) are related, because the *LCOS* can be thought as the average minimum price at which the electrical energy stored by the ESS must be sold in order to offset (i.e., $NPV = 0$) the total costs over its lifespan. It is worth noting that these indicators can be calculated by using different algorithms. The scheme used in this analysis is shown in Fig. 1, that presents the calculation structure of each term in Eqs. (1) and (2). Details are given in following sections.

2.2. Capital cost

The Unit Capital Cost (*UCC*), i.e. the capital expenditure per unit energy, was calculated as:

$$UCC = \frac{C_P + C_E + C_{BPL} + C_{ASS}}{E} \ [€\ kWh^{-1}] \quad (3)$$

where C_P are the costs of the materials and components related to the battery power (mainly, stacks), C_E are the costs of the materials and components related to the battery energy (mainly, electrolytes and tanks), C_{BPL} are the balance of plant costs (e.g. piping, pumps, instrumentation, power conditioning system, and battery management system) and C_{ASS} are the costs for battery assembling.

2.2.1. Power-related costs

The power of a *VFB* depends on the size of the stack and, therefore, the power costs C_P depend on the cost of the stack cost C_S. This cost depends on the cells number N_c and the cell active area A_c, according to the following Eq. [22]:

$$C_S = \left[f\left(c_m + c_{bp}\right)N_c + 2\left(c_{ed} + c_g\right)N_c + c_{ff}(N_c + 1) + 2(fc_{sh} + c_{cc})\right]A_c \quad (4)$$

where f is the material factor which takes into account material wasted during manufacturing and assembling of the stack, c_m, c_{bp}, c_{ed}, c_g, c_{ff} are the costs of the membrane, bipolar plate, electrodes, gaskets and flow-frame for each stack cell, while c_{sh} and c_{cc} are the costs of the stack heads and current collectors, respectively. N_c and A_c define the stack electric power P_S:

$$P_S = jA_cN_c[OCV - ASR\,j] \quad (5)$$

where j is the cell current density, $U = OCV–ASR\,j$ is the cell voltage, *OCV* is the cell Open Circuit Voltage and *ASR* is the cell area specific resistance. The *OCV* depends on the electrolytes concentration according to the Nernst equation, which can be rewritten in terms of the state of charge (*SOC*) of the battery as [34]:

$$OCV = E_0' - \frac{2\overline{R}T}{F} ln \frac{SOC}{1 - SOC} \quad (6)$$

E_0' is the corrected cell potential in standard condition at $SOC = 50\%$, $\overline{R}$ is the gas constant, T is the absolute temperature and F the Faraday

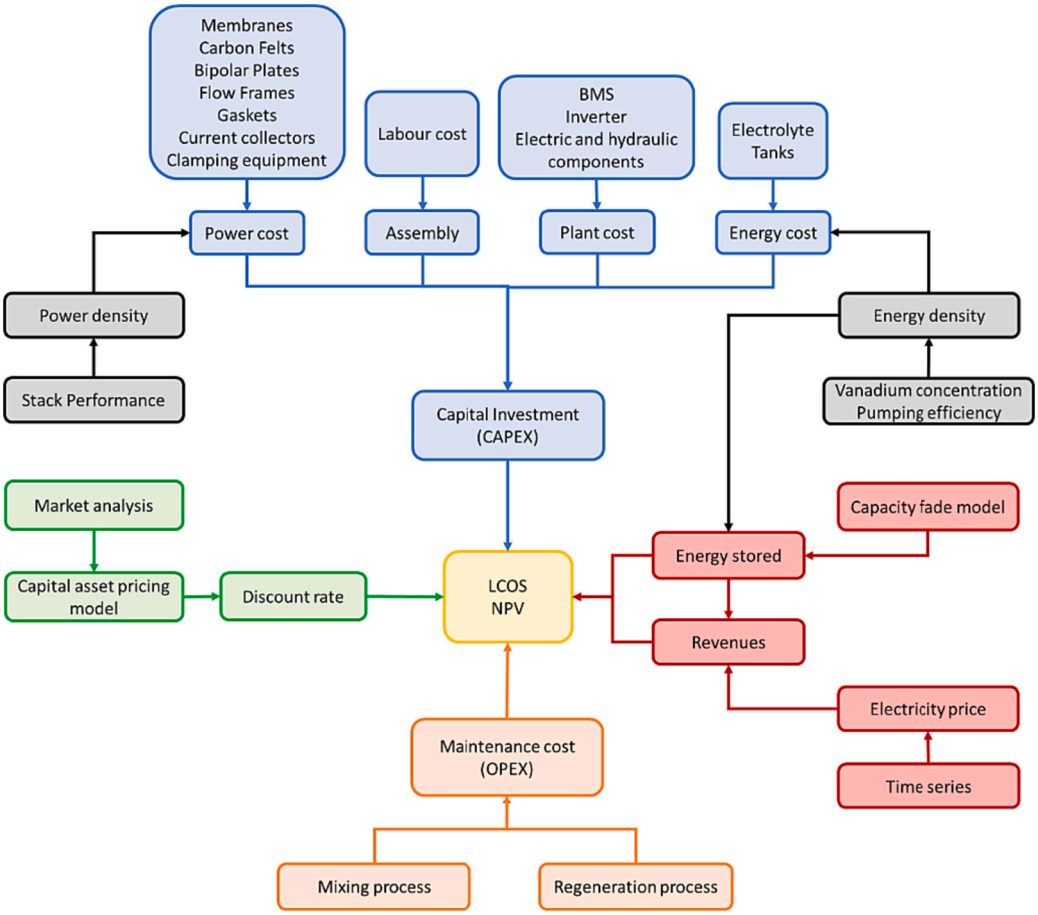

Fig. 1. Scheme of the economic analysis developed in this work in order to calculate both the levelized cost of storage (*LCOS*) and the net present value (*NPV*).

constant. The *ASR* depends on the electrode-membrane-bipolar plate architecture and also on the *SOC*, and in this work it was valued from the experimental data of the stack operated in an industrial–scale pilot system (*IS-VRFB*) at the Electrochemical Energy Storage and Conversion Laboratory of the University of Padua [35].

This stack consists of $N_c = 40$ cells with an active area $A_c = 30$ cm × 20 cm. The number of cells was chosen to limit the electric currents in the liquid electrolytes flowing in parallel to/from the cell homologous electrodes, named "shunt currents". Each cell consists of two 5.7–mm graphite felt electrodes (Beijing Great Wall, China), one Nafion 212 membrane and one flow-frame which encloses a sintered-graphite flat bipolar plate. The measured values of the *ASR* of each cell as function of the *SOC* in charge and discharge are reported in Fig. 2a [36]. Indeed, present state-of-the-art stacks have *ASR* lower that these, and around 0.8–1 Ω cm^2. Our investigation considered such better performance in the perspective analyses reported in Section 4, however retaining the previous dependence on *SOC*, to ensure a better accuracy to the model.

The dashed vertical lines in Fig. 2b-c-d correspond to the current densities $j = 100$ mA cm^{-2} in charge and $j = 120$ mA cm^{-2} in discharge, which are the maximum values at which the cell overpotentials do not involve dangerous side reactions and thus ensure long stack lifetime. Fig. 2c shows that, consistently with these current densities limits, the specific power densities delivered by the cells in charge and discharge are 0.16 W cm^{-2} and 0.10 W cm^{-2}, respectively [36]. Considering $N_c = 40$ and $A_c = 2000$ cm^2, the model provides powers in charge and discharge of 13 kW and 8 kW, respectively, as shown in Fig. 2d. These charging/discharging powers reduce to 10 kW and 6 kW at $A_c = 1500$ cm^2, 7 kW and 4 kW at $A_c = 1000$ cm^2, and to 3 kW and 2 kW at $A_c = 500$ cm^2. Stacks with active area in the range $A_c = 2000$–500 cm^2 are compatible with effective and competitive manufacturing and the previous values will be considered in the numerical analyses presented further on. Conversely, when the battery rated electric power P is much larger than the previous stack power figures P_S, instead of using a much larger stack that would pose major manufacturing issues, $N_S \approx P/P_s$ stacks are preferably installed and, in general terms, the power cost C_P is expressed as:

$$C_P = N_S C_S \tag{7}$$

2.2.2. Energy related costs

The volume V of each electrolyte depends on the energy E to be stored in the battery [30]:

$$V = \frac{E}{\overline{OCV}\,\Delta SOC\,F\,z\,M_v} \tag{8}$$

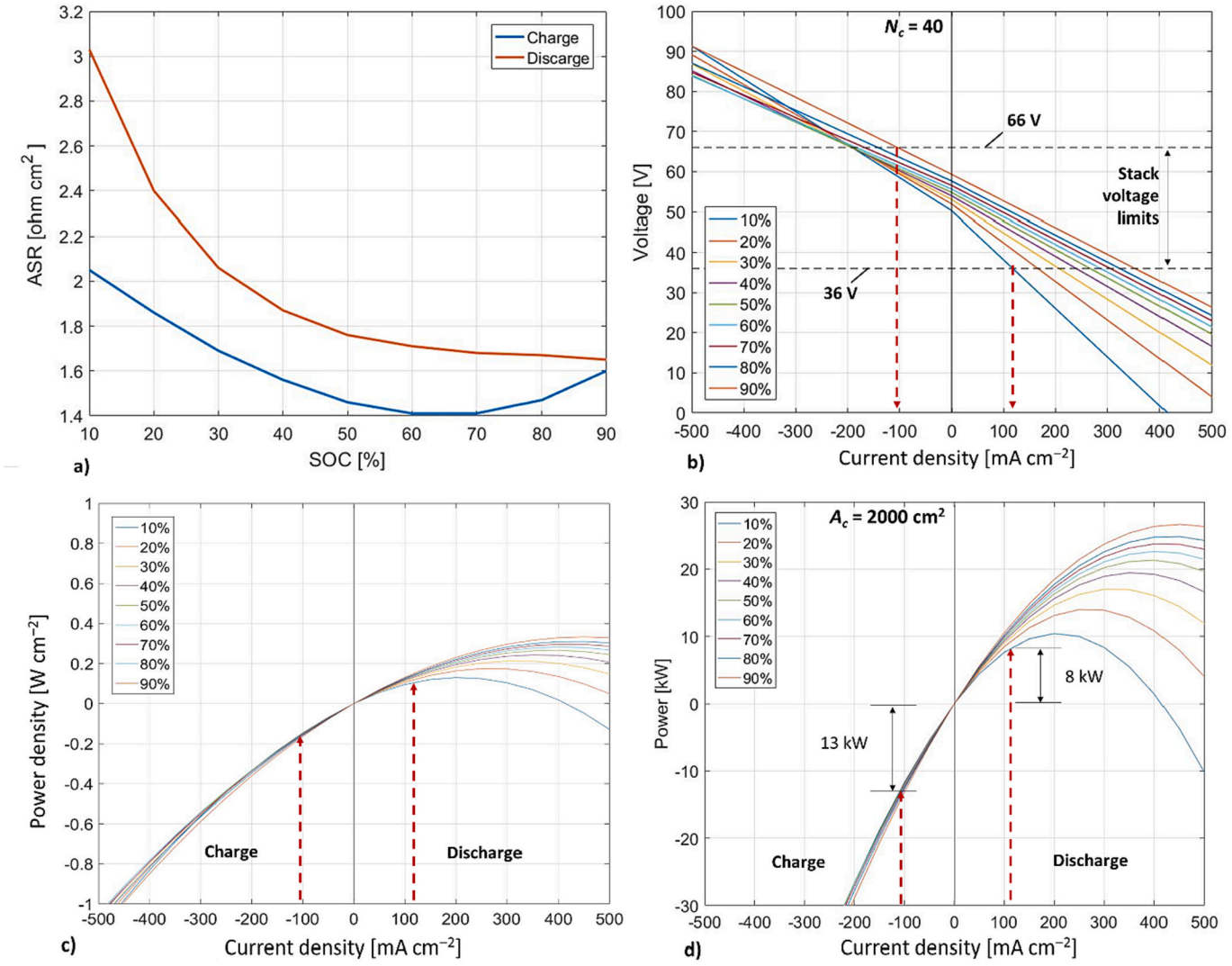

Fig. 2. a) Average charge and discharge Area Specific Resistance (*ASR*) of a cell of the *IS-VRFB* system operated at the University of Padua; b) Polarization curves in charge and discharge of the 40-cells stack with active area $A_c = 600$ cm^2 and *ASR* of Fig. 2a; c) Delivered cell power density vs. current density j and *SOC*; d) Delivered stack power vs. j and *SOC* in a stack with $N_c = 40$ and $A_c = 2000$ cm^2.

where $\Delta SOC = SOC_{max}–SOC_{min}$ is the state of charge variation in a complete discharge, z is the number of electrons transferred per electrochemical reactions ($z = 1$ in a *VFB*), M_V is the molar concentration of vanadium species, and $\overline{OCV}$ is the average open circuit voltage (i.e. the reversible cell voltage) during the process [22]:

$$\overline{OCV} = \frac{1}{\Delta SOC} \int_{SOC_{min}}^{SOC_{max}} OCV \, dSOC \tag{9}$$

SOC_{max} and SOC_{min} are never 100% and 0%, respectively, to avoid extreme conditions causing dangerous side reactions, and typical limiting values of *SOC* are instead 90% and 10%. Consequently, ΔSOC is never 100% and the depth of discharge (*DOD*) never reaches 100% so that not all nominal capacity is utilized, as also happens with closed batteries and hydrogen storage. The battery energy cost was considered to consist of the costs of electrolytes C_{el} and of the tanks C_t, both depending on the electrolyte volume V:

$$C_E = C_{el} + C_t = 2\, V\, c_{el} + 2\, k_t\, V\, c_t \tag{10}$$

The factor 2 accounts for both positive and negative electrolytes, c_{el} is the price of the electrolyte per unit volume, k_t is the tank volume increase with respect to electrolyte that was assumed to be 150% in this analysis [28] and c_t is a cost figure of the tank per volume capacity.

2.2.3. Balance of plant costs

In addition to the power and energy components described above, the operation of a *FB* requires other components and subsystems, constituting collectively the *BOP*. The hydraulic system consists of the piping (circulating the electrolytes between tanks and stack that is provided with maneuver valves) and two inverter-fed electrical pumps. The sizing of the pumps and piping depends on the electrolyte flowrates, which, in turn, are related to the battery electric power flow [37]. A Power Conditioning System (*PCS*) is needed to control the bidirectional electric power flow between the *FB* (operating in direct current) and the grid (typically in alternating current). Such operation is obtained with an ac/dc bidirectional static converter. A Battery Management System (*BMS*) supervises the whole system by acquiring and processing data from thermal, fluid-dynamic and electric probes and by providing the signals for controlling the electrolyte flowrates and the PCS electric power flow during charge and discharge, according to battery status variable and to the required power transfer. The *BMS* consists of a computer (or a microcomputer, or a programmable logic controller – *PLC*, …) with signal interfaces and dedicated software. Finally, *BMS* and *PCS* are complemented by sensors, circuit breakers, contactors, cables, alarms, circuitry [28]. Since the size of the plant depends on its power, the model assumes that the costs of the previous components and subsystem scale linearly with the battery power and therefore the *BOP* cost were expressed as follow:

$$C_{BOP} = (c_{BMS} + c_{PCS} + c_{ec} + c_h)P \tag{11}$$

where c_{BMS} is the specific costs of the *BMS*, c_{PCS} is the specific cost of the *PCS*, and c_{ec} and c_h are the specific cost of the electric circuitry and hydraulic system. The unit costs C_P, C_E, C_{BOP}, sum up to constitute the *UCC*, according to Eq. (3).

2.3. Operative costs

2.3.1. Capacity fade model

The performance and costs of *VFBs* over their lifespan depend on the capacity fade caused by side events such as: electrolyte diffusion across the membrane between the positive and negative cell electrodes, hydrogen evolution, electrode degradation, vanadium oxidation and vanadium salts precipitation. These effects cause different types of imbalances between the positive and negative electrolytes which call for rebalancing procedures. If extreme *SOC* are avoided and the battery is kept in an optimal temperature range, hydrogen evolution, electrode degradation and vanadium salts precipitation can be prevented. Conversely, electrolyte crossover cannot be avoided as long as membranes with zero ion permeability are missing, however it can be effectively counteracted by means of simple periodic electrolyte mixing, which can be performed in a total or partial mode [32]. Instead, mixing procedures have no effect on vanadium oxidation, which requires a regeneration process that makes use of special components/devices. Therefore, in order to rebalance the vanadium concentrations, both electrolyte mixing and regenerating process may be required [38]. K.E. Rodby et al. provide a good physical model to simulate the capacity fade due to electrolyte imbalances [29] that uses two fade rates expressing the relative capacity loss per month [% month^{-1}]: FR_{cr} due to crossover and FR_{ox} due to vanadium oxidation. A graphical representation of the model is shown in Fig. 3. It assumes that the *VFB* energy capacity relative to nominal values $E_{\%}$ starts at 100% and the system undergoes one charge/discharge cycle per day. Due to crossover fade rate FR_{cr}, the energy capacity gradually decreases and when it reaches the threshold $E_{\%\min} = 80\%$, a mixing process is activated to restore the capacity to the maximum possible value $E_{\%max}$, which in the while has decreased with rate FR_{ox} due to oxidation. When $E_{\%max}$ reduces to $E_{\%min}$, a regenerating process is applied to restore the initial capacity, i.e. $E_{\%max} = 100\%$. The evolution of Fig. 3 corresponds to FR_{cr} and FR_{ox} requiring 20 mixing and one regenerating operations per year, respectively, consistently with data reported in the literature [29,39], so that, after one year of operation and 20 mixing process, the $E_{\%max}$ matches the $E_{\%\min}$. In this condition the mixing process is no more effective and a regenerating process is needed to restore 100% capacity, making the battery operative for another year.

2.4. Exercise and maintenance costs

Operative cost includes battery exercise and the maintenance procedures preserving the battery operativity. According to the scheme shown in Fig. 3, $n_{mix} = 20$ mixing processes and $n_{regx} = 1$ regeneration process are run per year, to recover the initial battery capacity. The cost of the former does is given by the energy lost in the mixing procedure. Conversely, regeneration requires a periodical external intervention which represent a cost during the lifespan of the battery. The expenditure of all maintenance processes performed in a year originates from the energy consumed in the mixing processes E_{mix} and the cost for regenerating the electrolytes. It was assumed that this regenerating process was performed by means of chemical reducing agents such as ethanol or oxalic acid [29] that was bought as paid service at a cost c_{reg} [29]. The resulting *OPEX* is:

$$OPEX_i = c_e\, n_{mix}\, E_{mix} + n_{reg}\, c_{reg} E \tag{12}$$

where n_{mix} and n_{reg} are the number of times which the mixing and the regenerating process take place in a year respectively. The electrical energy E_{mix} requested to restore a suitable *SOC* both in the positive and negative electrolyte after the mixing process must be bought from the grid and, to reduce its cost and maximize profitability, the process could be performed when the grid electricity cost c_e is minimum. Alternatively, this energy can be provided by an own renewable source, so that the mixing energy, rather than a cost, was considered a lack of profit at a price p_e. The unit operating cost (*UOC*), i.e. the operative expenditure per unit energy, is obtained from the *OPEX* as:

$$UOC_i = \frac{OPEX_i}{E} \tag{13}$$

3. Costs and technical data

3.1. Capital and operational costs

Table 2 lists the cost data communicated by suppliers, which were

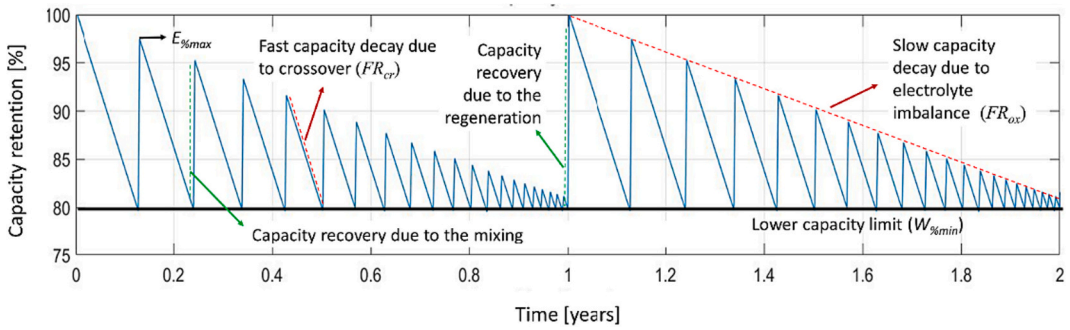

Fig. 3. Graphical representation of the battery capacity as a function of time according to Rodby's model [32]. The capacity decay due to crossover is faster than that caused by oxidation, because $FR_{cr} > FR_{ox}$. In this schematization, $E_{\%min} = 80\%$, the mixing process is run 20 times in a year and the regenerating procedure once a year.

used to calculate the power and energy related costs. Table 3 lists cost data used to compute the *BOP* costs, among which the specific costs per unit of power of *PCS* ac/dc converter, electric components and circuity and piping were retrieved in the literature [14,22,23,40], whereas the specific costs of pumps and *BMS* were obtained by interpolating quotations provided by different producers by means of:

$$\frac{C_a}{C_b} = \left(\frac{P_a}{P_b}\right)^{\alpha} \tag{14}$$

where $P_{a,b}$ are the *VFB* rated powers, $C_{a,b}$ are the costs of the components sized for such *VFBs* and α is an interpolation exponent. The interpolation exponent α reported in Table 3 were determined using two couples of known values ($C_{a,b}$,$P_{a,b}$), after which Eq. (14) with a known (C,P) couple was used to estimate the unknown cost C_x of components sized for a *VFB* with a given rated power P_x. For the costs for battery assembling of Eq. (3) was assumed as $C_{ASS} = 10\%$ of the expenditure in materials and components.

In an initial analysis, the *RTE* of Eqs. (1) and (2) was assumed as $\eta_{RT} = 75\%$, that is a prudential figure deduced from published experimental values accounting for all *VFB* losses (including shunt currents, hydraulic and auxiliary system losses) [35]. A better figure $\eta_{RT} = 85\%$is used in the perspective analysis.

3.2. Economic parameters

Table 4 lists the most important techno-economic parameter used in the analyses. The number of cells per stack is 40, the same value of the stack experimented in [36] and a typical value of industrial stacks. To evaluate the profitability of *VFB* systems, a lifespan must be assumed. This is not usually the working life of the equipment, nor it is the time over which the capital investment is recovered. It is rather a period over which the profitability of different projects can be compared. According to the literature and datasheets of marketed systems, *VFBs* can operate over 20,000 charge-discharge cycles, which corresponds to >50 years of operative life if one cycle per day is executed. However, since no *VFB* plant has been operated over such a long period, we adopted a conservative choice assuming a lifespan of 20 years, with one charge/discharge cycle per day. Electricity prices vary from country to country and this analysis considered the prices in Italy, where the plant was assumed to be located. Price estimations were based on the PUN (Italian acronym for National Single Price), which is the wholesale reference price of electricity at the Italian Power Exchange, obtained as the national weighted average of the local sales prices of electricity in each hour for every day. [41,42]. PUN daily curves are shown in Fig. 4. Figures a), b), c) and d) for the month of April 2005, 2010, 2015 and 2023. They highlight that the electricity prices remained in a steady range in the past years, with daily swings up to 70–80 € kWh^{-1}, but now their dynamics is changing quickly, presenting daily swings in excess of 200 € kWh^{-1} with minima between 9:00 and 18:00. This is a known behavior, named *Duck Curve*, typical of grids with a high penetration of photovoltaic energy. Based on these evidences, it was assumed to profit of these increasing price swings to adopt an *arbitrage service* strategy that consists in charging from the grid in hours when the energy is bought at low cost c_e and discharging when the energy is sold to the grid at high price p_e. In order to compare cash flows from costs and revenues occurring at different future times, their values must be evaluated at the same time (usually the present time), by means of the discount rate r that

Table 2
Cost parameters for VFB power and energy components.

Component	Cost	Unit
Membrane	200	€ m^{-2}
Porous electrode	100	€ m^{-2}
Bipolar plate	100	€ m^{-2}
Half–flow frame	50	€ m^{-2}
Gasket	100	€ m^{-2}
Current collector	170	€ m^{-2}
Stack head	1000	€ m^{-2}
Clamping equipment price	200	€ $stack^{-1}$
Vanadium electrolyte	5	€ L^{-1}
Tank	300	€ m^{-3}

Table 3
Cost parameters for the BOP [20,26,27,43].

Component	Cost	Unit
PCS ac/dc converter	150	€ kW^{-1}
Electric system	50	€ kW^{-1}
Piping and fittings	100	€ kW^{-1}
Pumps specific cost C/P^{α} – Eq. (14)	200	€ $kW^{-\alpha}$
Pumps interpolation exponent α	0.60	
BMS specific cost C/P^{α} – Eq. (14)	800	€ $kW^{-\alpha}$
BMS interpolation exponent α	0.76	

Table 4
Techno-economic parameters used in the prudential profitability analysis.

Parameter	Symbol	Value	Unit
Number of cells in a stack	N_c	40	–
Number of mixing processes in a year	n_{mix}	20	–
Number of regeneration processes in a year	n_{reg}	1	–
Unit cost of regenerating process	c_{reg}	10	€ kWh^{-1}
Electricity sale price	p_e	200	€ MWh^{-1}
Electricity purchase price	c_e	100	€ MWh^{-1}
Inflation rate	i	1	%
Discount rate	r	10.08	%
Plant lifespan	y	20	year
Cycle per day	–	1	–
Round trip efficiency	η_{RT}	75	%
State of charge variation	ΔSOC	80	%

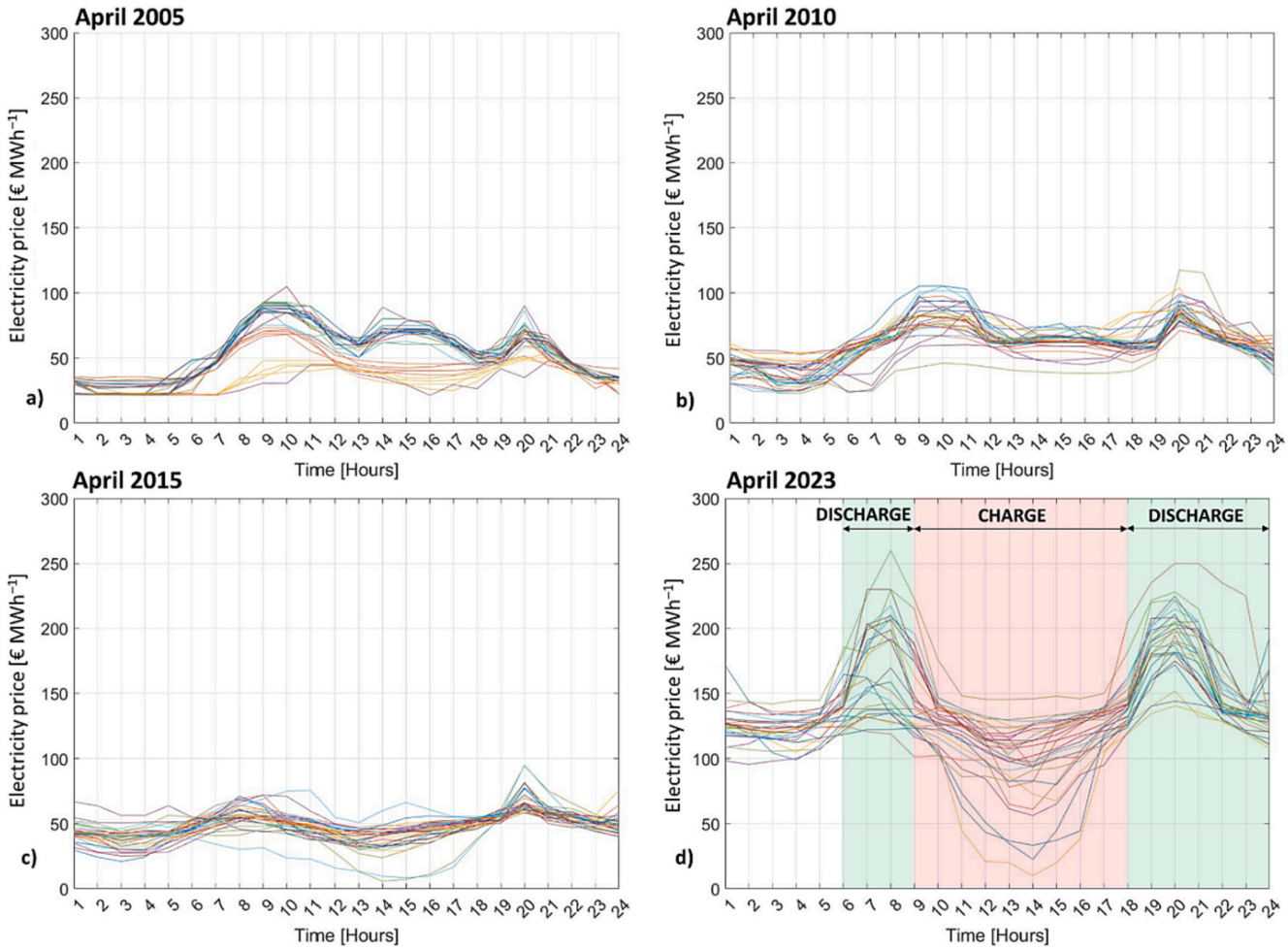

Fig. 4. Daily electricity price in the month of April in different years: a) 2005; b) 2010; c) 2015; d) 2023.

allows to compute the present values of future expenses and revenues occurring year after years during the battery lifespan. This values, constitutes a cost of capital adjusted for technology-inherent risks, as expressed by Capital Asset Pricing Model (CAPM) [43]:

$$r = r_f + \beta\,\mathrm{MRP} \tag{15}$$

where r_f is the risk-free interest rate, such as the rate of very short-term government bonds of absolutely reliable countries. β is the investment systematic risk, namely it is a measure of how much the investment is risky with respect to the portfolio of a reference market, in this case dealing with energy technologies.

If $\beta > 1$ the investment is more risk, or more volatile, than the market, while if $\beta < 1$ the investment is safer, or less volatile, than the market. In the model we use the unlevered beta, that measures the market risk of a company without the impact of debt. *MRP* is the Market Risk Premium, so that βMRP accounts for the additional risk that an investor takes when he decides to invest in a given technology.

In this analysis, an average of the last 10 years return of the Italian BTP-10y (10 years state bonds) as published by the Italian Central Bank was used for the risk-free interest rate, i.e. $r_f = 2.67\%$ [44]. The used value of β corresponds to the average unlevered beta values weighted by installed capacity share of five world-class *VFB* manufacturers (Table 5). These companies were chosen because: 1) they installed at least 10 MWh of *VFBs* worldwide; 2) their financial indicators were available online. Finally, the used Italian market risk premium is $MRP = 6\%$ [45]. By using these data, Eq. (20) yields $r = 9.12\%$, that can be considered a prudential assumption for the present model.

Table 5
Beta values of some big *VFBs* manufacturers [19,44,46].

Company	Country	Capacity share	Unlevered beta
Invinity	UK–USA	17%	2.50
Sumitomo	Japan	42%	0.89
Largo	Canada	3%	0.86
Shanghai Electric	China	18%	0.64
CellCube (Bushveld)	Austria–South Africa	20%	0.68

Evaluating *EOL* costs of Eq. (1) is an awkward question, that some comparative analyses resolve in an uncritical and undifferentiated manner putting it at zero for all considered technologies [18,19], so that the results benefit those which have major disposal and recycling issues (e.g. Li-ion batteries) and penalize those which may have a residual market value. In particular, published life cycle assessments show that *VFBs* at end of life maintain 70% of their value and only 30% of the component investment must be spent to obtain a second life battery [13,23,47]. In addition, the vanadium electrolyte after regeneration preserves its operative value because it is not affected by cross-contamination and aging effects. However, no market quotations are available at present for vanadium reselling, so that in a prudential analysis it was assumed *EOL* cost equal to zero, consistently with most literature [13,23]. A more favorable hypothesis is made in the perspective analysis.

4. Results

4.1. LCOS and NPV with prudential assumptions

The model has been applied to compute the *VFBs* levelized cost of storage (*LCOS*) and the unit capital cost (*UCC,* i.e. investment per unit energy) as functions of the battery energy to power ratio *E/P* and single stack power P_S (Fig. 5). The technical and economical parameters of the previous Tables have been used in this simulation, in order to obtain prudential present-day evaluations. Both *LCOS* and *UCC* decreases as *E/P* increases. At *E/P* = 2 h, the model yielded *UCC* = 800–900 € kWh^{-1} and *LCOS* = 0.50–0.55 € kWh^{-1} cycle^{-1}, whereas at *E/P* = 10 h it was obtained *UCC* = 350–380 € kWh^{-1} and *LCOS* = 0.29–0.32 € kWh^{-1} cycle^{-1}, i.e. the former reduced by ca. 48% and the latter by ca. 30% as *E/P* increases from 2 to 10 h. The differences of *UCC* and *LCOS* among *VFBs* having the same *E/P* and different P_S is larger at small *E/P* and reduce as *E/P* increases. However, the stack power P_S impacts on the number of stacks used to achieve a high plant power *P*, e.g. a storage plant rated 1 MW / 10 MWh can be built with 500 stacks rated 2 kW or 125 stacks rated 8-kW, with small differences in terms of *UCC* and *LCOS*, but the different numbers of stacks may have a major impact on plant complexity and occupied area.

Fig. 5-Inset shows the results for the net present values (*NPV*), which evaluates the profitability of the investment, as a function of *UCC*. It shows that *NPV* = 0 at *UCC* = 200 € kWh^{-1}, namely this is the break-even-point where the present values of total costs equate the present values of total revenues and no economic result is obtained. Every *UCC* < 200 € kWh^{-1} yields *NPV* > 0, i.e. the investment is profitable, whereas every *UCC* > 200 € kWh^{-1} yields *NPV* < 0, i.e. the investment is at loss. Fig. 5-Inset reports in abscissa the *UCC* values of Fig. 5, all falling in the loss region, indicating that the investment in *VFBs* is never profitable with the prudential parameter scenario assumed in this first simulation. However, these results strongly depend on the assumed values of the model parameters as shown further on.

4.2. LCOS and NPV with perspective assumptions

Some of the parameters involved in the model are related to the system performance, such as power density and efficiency, while others depend on the market conditions, such as component costs, electricity price and discount rate. The values of these parameters are evolving and some *VFB* systems recently marketized already present better performance and thus better figures for such parameters while other are expected to improve in the near future. Also, some economic parameters are expected to evolve in such a way to provide better profitability. Thus, it makes sense to estimate the economic *KPIs* assuming improved perspective parameters values to figure the profitability and competitiveness to which *VFBs* are heading in the next future. Regarding technical parameters, the effect of power density, *RTE* and *ΔSOC* were investigated. Although other parameters also affect the performance, e.g. the vanadium concentration in the electrolyte, only the variations of these three technical parameters were considered in the perspective analysis because they are expected to undergo major improvements. Indeed, the power density can be improved by reducing the cell resistance. As already stated, the present state-of-the-art stacks present *ASR* ≈ 0.8–1 Ω cm^2, i.e. ca. 60% of the values of Fig. 2, thanks to different stack technological improvements [48,49]. Such lower *ASR* allows to operate at current density above 200 mA cm^{-2} in both charge and

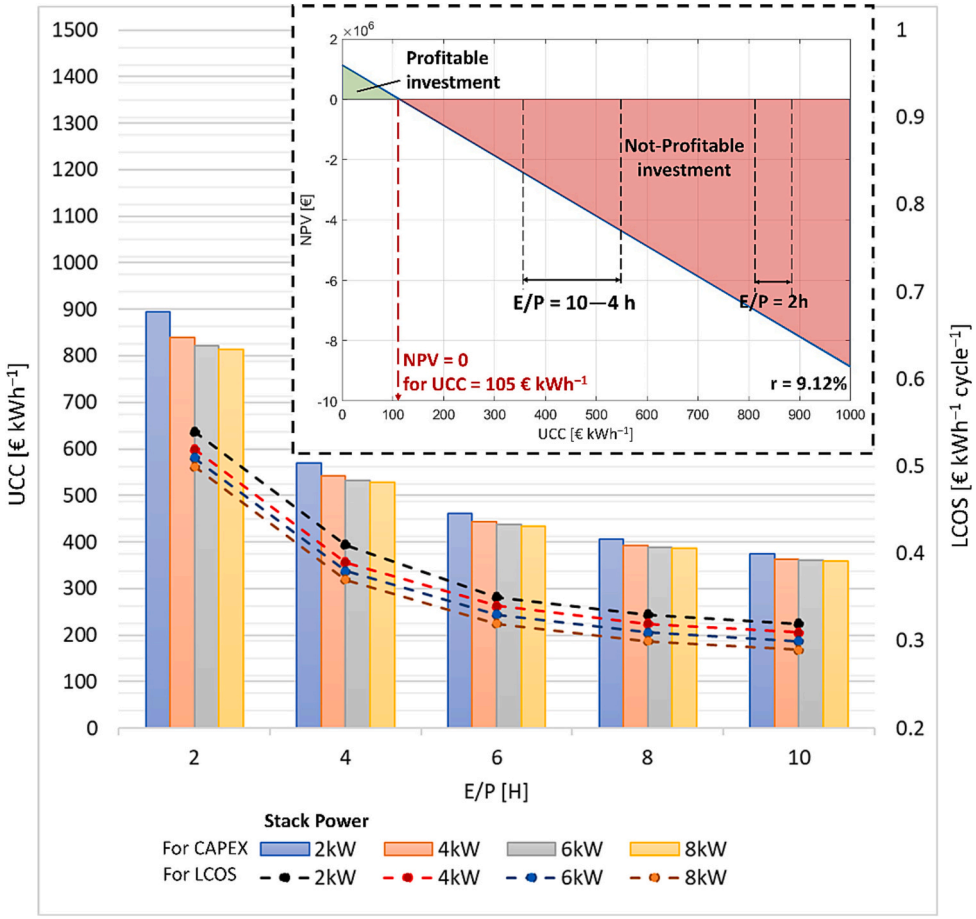

Fig. 5. *UCC* and *LCOS* vs. *E/P* for 4 stack powers given by 4 cell areas: 500 cm^2, 1000 cm^2, 1500 cm^2, 2000 cm^2. **Inset**: *NPV* vs. *UCC*. The *UCC* values correspond to *E/P* ranging from 2 to 10 h. All *UCC* values obtained in the model and shown in Fig. 5 fall in the non-profitability area;

discharge within the same cell overpotential limits of Fig. 2 (Fig. 6a) thus achieving a maximum power density of 0.25 W cm^{-2} in discharge and 0.4 W cm^{-2} in charge (Fig. 6b). Consequently, the power delivered by one stack of $N_c = 40$ cells with an active area $A_c = 2000$ cm^2 increases to $P_S = 20$ kW, with correspondingly increased power density.

Finally, a wider ΔSOC can be reached thanks to a more efficient mixing between inlet and outlet electrolytes in the tanks. This can be achieved with advanced tank designs combined with a dedicated flow-rate management [50]. The histogram of Fig. 6c shows the effects on *UCC*, considering a *VFB* system with $E/P = 10$ h. The first bin refers to the reference case taken from *IS-VRFB* measurements, while the second, third and fourth bins present the *UCC* reductions due to the above improvements in *RTE*, ΔSOC and power density, respectively.

According to the model, improving power density by reducing *ASR* values as 50% has a major effect of −12% on the *UCC*, while ΔSOC and the vanadium molarity acts each as −8%. The last bin shows the combined effect of all the three changes, resulting in a *UCC* of 261 € kWh^{-1}. Some costs items do not affect directly the *UCC* but only the *LCOS*. An example is the number N_{reg} of regenerating processes, which contributes to the *OPEX* as in Eq. (12). According to the literature, some *VFBs* are in operation since over ten years without requiring regenerating processes, differently from the assumption adopted in Section 2.3 [51]. For this reason, it interesting assuming a reduced number of regenerating processes in 20 years of lifespan. In particular, a regenerating process every five years was considered, so that the total regenerating processes over the lifespan of 20 years is $N_{reg} = 4$ (i.e., $n_{re} = 0.2$). As regards the discount rate, most researches consider a value lower than $r = 9.12\%$ here assumed [23]. A value $r = 7\%$ was considered, which is consistent with a *CAPEX* financed 70% by equities and 30% by debt and with a reduced investment risk expected as the technology consolidates. Another important parameter is the electricity price. Since the percentage of renewable energy production will increase, it is plausible that the *Duck Curve* will accentuate in the future so that a larger difference between selling price p_e and a purchasing price c_e becomes plausible. To investigate this effect, a selling price $p_e = 250$ € MWh^{-1} and a purchase cost $c_e = 70$ € MWh^{-1} were considered (Fig. 7a). Also, *RTE* impacts on the *LCOS* and *NPV*, according to Eqs. (1) and (2).

The *RTE* can be improved, notably, by minimizing shunt current

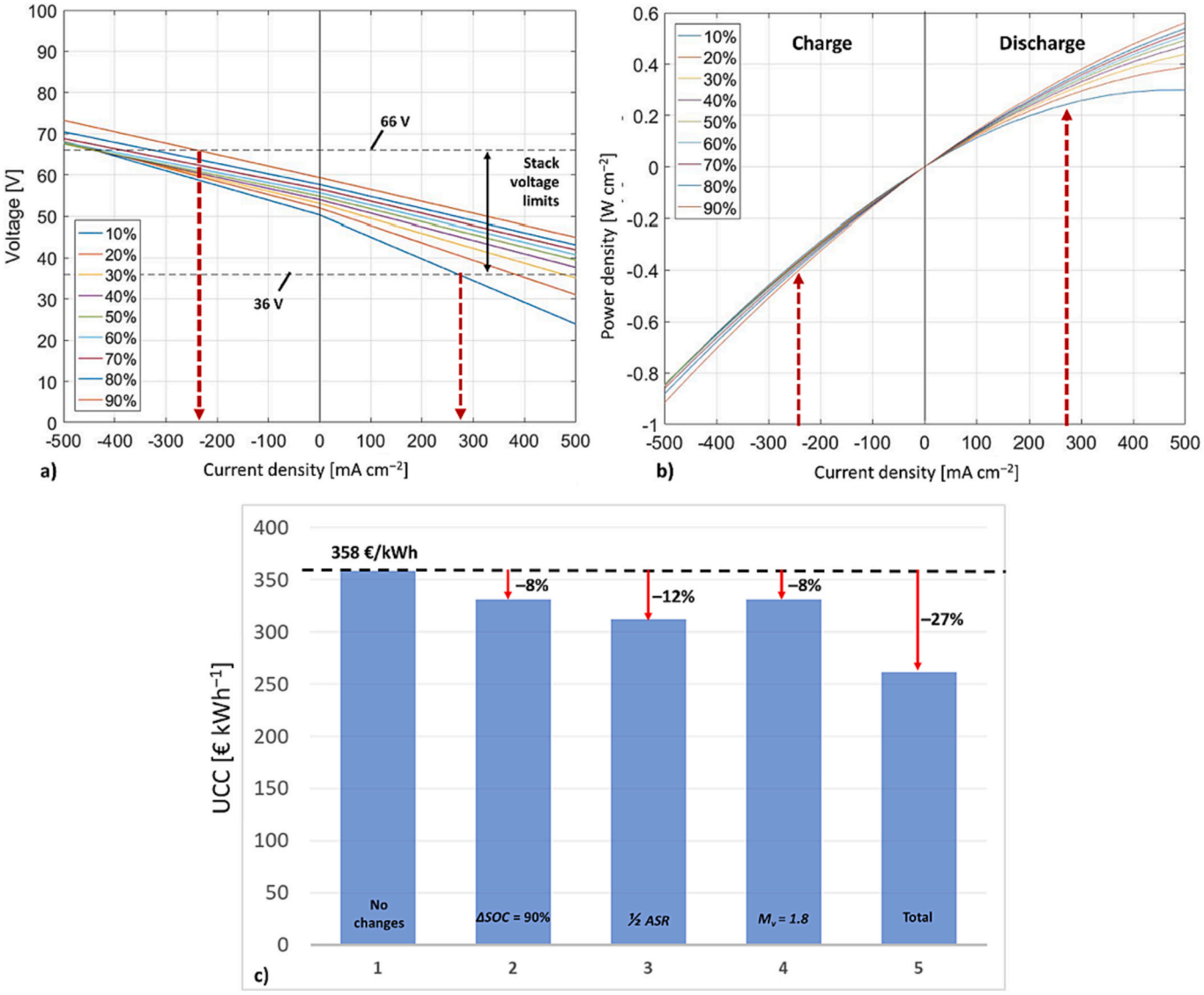

Fig. 6. Performance of a 40-cells stack with $A_c = 2000$ cm^2 and $ASR = 50\%$ lower than Fig. 2c vs. current density j at different *SOCs*. a) Polarization curves in charge and discharge; b) delivered cell power density. c) Sensitivity analysis on the *UCC* of a *VFB* system with $E/P = 10$ h by technical parameter improvements: 1) reference *UCC* with no improvement; 2) *UCC* with a ΔSOC increase of 10% (thus reaching 90%); 3) *UCC* with *ASR* values reduced by the half respect to Fig. 2c; 4) *UCC* with a vanadium molar concentration $M_v = 1.8$ M; 5) *UCC* after the cumulative effects of all three improvements.

losses and by dynamically optimizing the electrolyte flow rate [52]. Typically, shunt currents affect the *RTE* by ca. 10%, so that their reduction can produce a major impact on the operating costs. A dynamically optimized flow rate can increase the *RTE* of about 3–4% [52,53]. Furthermore, an analysis was carried to investigate how *EOL* economic events may impact on the *LCOS*. In the case of *VFB EOL*, the *BOP* and stacks disposal produce a cost while the vanadium electrolyte preserves its value and can produce a revenue. In the computation it was assumed that disposal cost was 10% of C_{BOP} and C_P, while the electrolyte could be resold at 70% of the purchase price, i.e. a present 3.5 € $^{-1}$. Fig. 7b shows the effects produced by all previous perspective parameter variations on the *LCOS* of a *VFB* with $E/P = 10$ h.

The first bin represents the reference case, while the others represent, from left to right, the *LCOS* reduced for lower number of regenerating processes, changed electricity prices, reduced discount rate, improved *RTE*, and *EOL* economic events. The decreases were respectively 10%, 7%, 7%, 3%, and 20%; i.e., electrolyte resale produced the major effect. The last bin shows the cumulative effects of all these beneficial changes together. All these effects impact on the investment cost and on the profitability of a *VFB* systems, as shown in Fig. 8, which shows the resulting *UCC* and the *LCOS* values assuming the most profitable parameter configuration previously considered, i.e. $N_r = 4$, $r = 7\%$, $p_e = 250$ € MWh^{-1}, $c_e = 75$ € MWh^{-1}, power density of 0.25 W cm^{-2}, $RTE = 85\%$, $\Delta SOC = 90\%$ and *EOL* economic events. The result is that at $E/P = 2$ h, the values of $UCC = 530$–570 € kWh^{-1} and $LCOS = 0.23$–0.24 € kWh^{-1} cycle^{-11}, whereas at $E/P = 10$ h, $UCC = 260$–270€ kWh^{-1} and $LCOS = 0.13$ € kWh^{-1} cycle^{-1}. With this parameter scenario *VFBs* present the break-even-point at $UCC = 500$ € kWh^{-1} and the investment is profitable for E/P in the range of 4–10 h, as shown in Fig. 8-Inset.

A final consideration regards the life cycles of *VFBs*. In all previous analyses it was retained the assumption of one cycle per day over 20 years of lifespan which means a total of 7300 cycles, namely much less of the life cycles specified by *VFB* manufactures who typically promise 20,000 cycles. In order to evaluate how a longer lifetime may impact on the economic *KPIs*, it was considered a life of 14,600 cycles in a *VFB* rated 1 MW with E/P from 2 to 10 h, obtaining the results of Fig. 9, i.e.

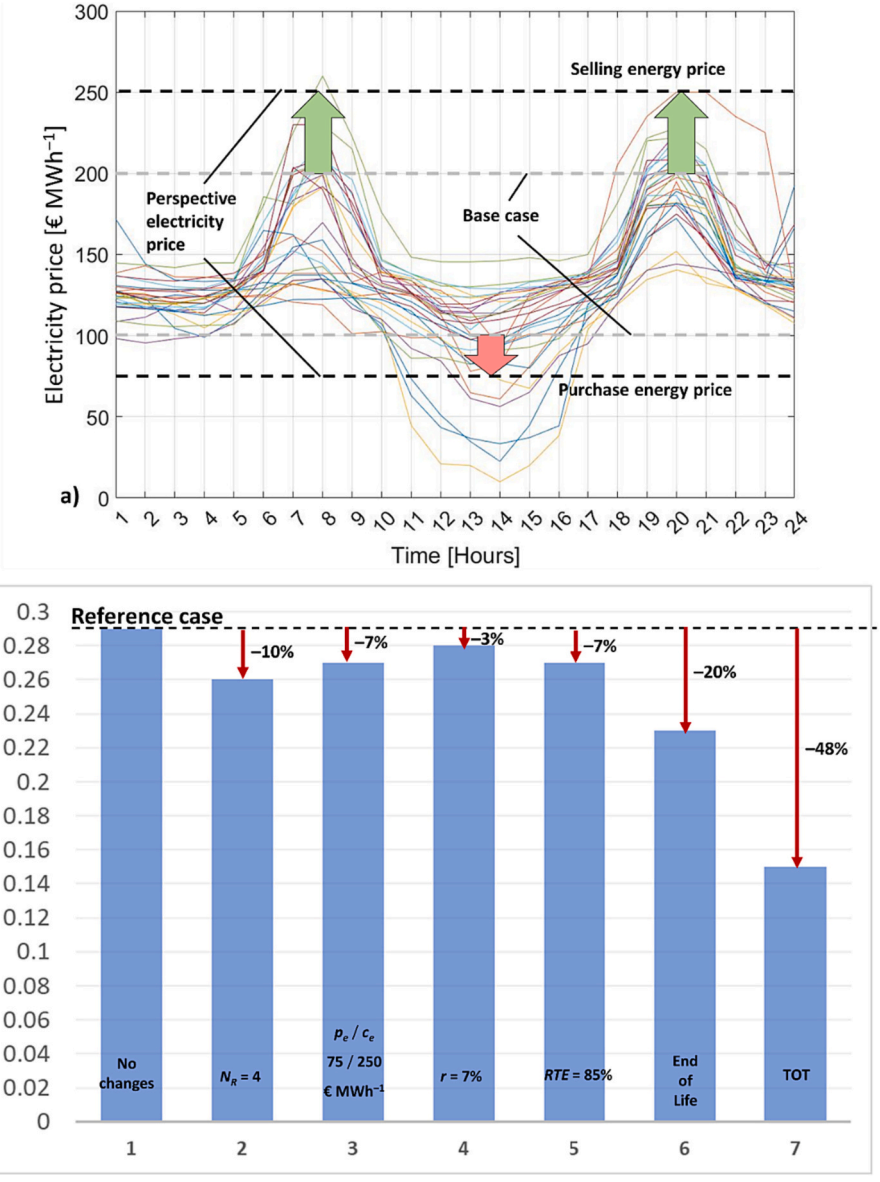

Fig. 7. a) Perspective electricity price used in the perspective analysis, with high selling price $p_e = 250$ € MWh^{-1} during discharge and low purchase price $c_e = 75$ € MWh^{-1} during charge; b) Sensitivity analysis on the *LCOS* of a *VFB* with a E/P = 10 h: 1) reference *LCOS* with no changes; 2) *LCOS* with $N_{reg} = 4$; 3) *LCOS* with $p_e = 250$ € MWh^{-1} and $c_e = 75$ € MWh^{-1}; 4) *LCOS* with a discount rate $r = 7\%$; 5) *LCOS* with $RTE = 85\%$; 6) *LCOS* considering and *EOL* events; 7) *LCOS* resulting from the cumulative effects of all these changes.

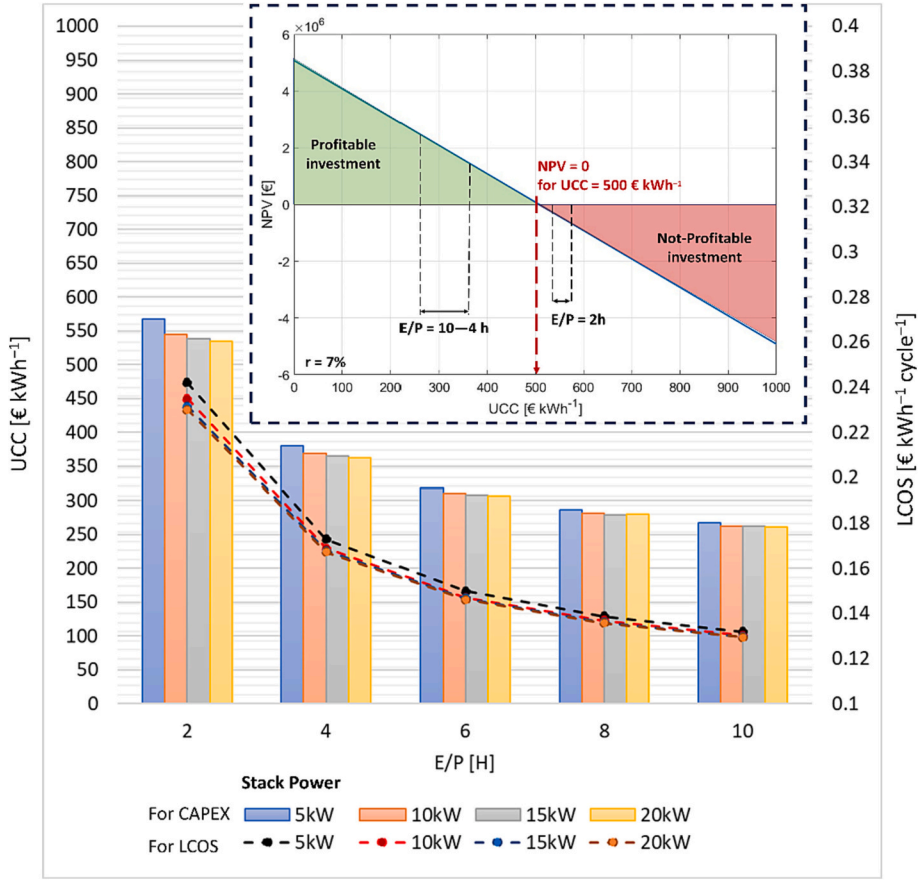

Fig. 8. Effect of the perspective analysis: *UCC* and *LCOS* vs. *E/P* for 4 stack powers given by 4 cell area: 500 cm^2, 1000 cm^2, 1500 cm^2, 2000 cm^2. **Inset**: Sensitivity of *NPV* as a function of *UCC* for *E/P* ranging 2 to 10 h, assuming the most profitable configuration. *E/P* values correspondent to those of Fig. 10a show that $E/P > 2$ h are profitable.

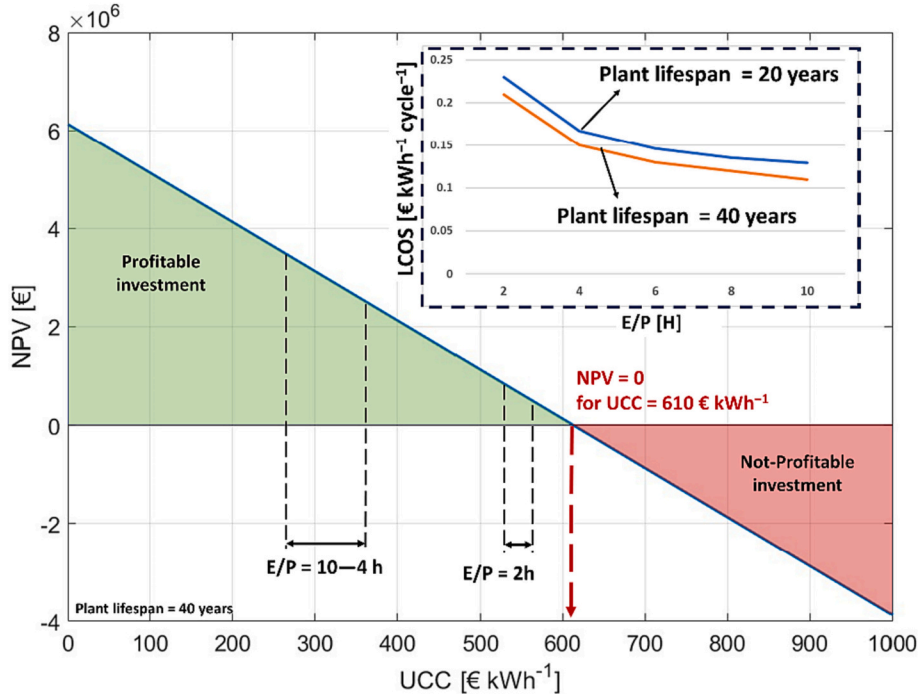

Fig. 9. Effect of the life extended to 14,600 cycles in a system rated 1 MW: the beak-even point in *NPV* increases to 610 € kWh^{-1} **Inset:** *LCOS* reduces by ca. 0.02 € kWh^{-1} $cycle^{-1}$.

LCOS reduced by ca. 0.02 € kWh^{-1} $cycle^{-1}$ and approaching 0.11 € kWh^{-1} $cycle^{-1}$. Consistently, the area of profitability in the NPV diagram expands with a break-even point at ca. 610 € kWh^{-1}.

5. Conclusions

A techno-economic assessment of Vanadium Flow Batteries was performed considering a lifespan of 20 years with a charge/discharge cycle per day, using the experimental data taken from industrial-size plants and literature. Each component affecting the capital and operative costs was analyzed and the impact of side phenomena on capacity losses was considered. Relevant economic parameters were taken from real market data: discount rate was calculated based on the CAPM to account for real market conditions; the electricity price follows an arbitrage strategy to profit of the daily price fluctuations taken from the historical data of the Italian energy market. The resulting values are: a discount rate of 9.12% and electricity prices of 200 € MWh^{-1} in selling and of 100 € MWh^{-1} in buying. *UCC* and *LCOS* were calculated for different system power and energy ratings. At $E/P = 2$ h, the values of *UCC* and *LCOS* were in the range of 800–900 € kWh^{-1} and 0.50–0.55 € kWh^{-1} $cycle^{-1}$, respectively, whereas at $E/P = 10$ h they reduced to 350–380 € kWh^{-1} and 0.29–0.32 € kWh^{-1} $cycle^{-1}$, respectively. In addition, a *NPV* analysis was carried out in order to evaluate whether these capital costs could provide a profit. The analysis suggests that only at $UCC < 105$ € kWh^{-1} the break-even point ($NPV = 0$) was reached. The result is that in the assumed techno-economic scenario *VFBs* were not profitable for every considered *E/P*. A perspective analysis was developed to reveal when *VFBs* can become profitable. Different screenings were made on both technical and economic parameters.

At a technical level, a power density of 0.25 W cm^{-2}, a $RTE = 85\%$, a $\Delta SOC = 90\%$, and a reduced number of regenerating processes in the lifespan ($N_{reg} = 4$) were considered. Regarding the economic parameters, a discount rate of 7% was assumed, an electricity selling price of 250 € MWh^{-1} and a purchasing price of 75 € MWh^{-1} were used, compatible with a more pronounced *Duck Curve* of the daily electricity price, induced by the expansion of renewable energy sources expected in the near future.

Regarding the *EOL* of the battery, it was considered an electrolyte reselling price of 3.5 € L^{-1} and the *BOP* and the stacks disposed cost of 10% of the initial cost. Under this scenario, the system costs decreased considerably: at $E/P = 2$ h, the *UCC* and *LCOS* ranged as 530–570 € kWh^{-1} and 0.23–0.24 € kWh^{-1} $cycle^{-1}$, respectively, whereas at $E/P = 10$ h, the *UCC* ranges as 260–270 € kWh^{-1} and *LCOS* around 0.13 € kWh^{-1} $cycle^{-1}$. The latter figures made *VFBs* profitable for *E/P* in the range of 4–10 h. As a final comment, it is worth noting that *VFBs* are sold for extremely long cycle lives, which extend beyond 20 years of operation, unparalleled by other types of batteries. The analysis at doubled number of cycles (14,600 cycles) revealed an additional improvement of both LCOS, down to 0,11 € kWh^{-1} $cycle^{-1}$, and NPV, with break even at 610 € kWh^{-1}.

CRediT authorship contribution statement

Nicola Poli: Writing – original draft, Validation, Methodology, Formal analysis. **Cinzia Bonaldo:** Writing – original draft, Methodology, Formal analysis. **Michele Moretto:** Supervision, Conceptualization. **Massimo Guarnieri:** Writing – review & editing, Supervision, Funding acquisition, Conceptualization.

Declaration of competing interest

The authors declare that they have no known competing financial interests or personal relationships that could have appeared to influence the work reported in this paper.

Data availability

Data will be made available on request.

Acknowledgments

This work was supported by funding from the project “Grid-optimized Vanadium Flow Batteries: Architecture, Interconnection and Economic Factors” (GUAR_RICERCALASCITOLEVI 20_01), within the 2019 Research Program of the Interdepartmental Centre Giorgio Levi Cases for Energy Economics and Technology of University of Padua and from the project “Holistic approach to EneRgy-efficient smart nanOGRIDS – HEROGRIDS” within (PRIN 2017 2017WA5ZT3) within the Italian MUR 2017 PRIN program.

References

[1] Mehrjerdi H. Simultaneous load leveling and voltage profile improvement in distribution networks by optimal battery storage planning. Energy Aug. 2019;181:916–26. https://doi.org/10.1016/J.ENERGY.2019.06.021.
[2] Turker B, et al. Utilizing a vanadium redox flow battery to avoid wind power deviation penalties in an electricity market. Energ Conver Manage Dec. 2013;76:1150–7. https://doi.org/10.1016/J.ENCONMAN.2013.09.014.
[3] Dowling JA, et al. Role of long-duration energy storage in variable renewable electricity systems. Joule Sep. 2020;4(9):1907–28. https://doi.org/10.1016/J.JOULE.2020.07.007/ATTACHMENT/CE7FB308-32A7-4A52-82DE-2E9757A3431B/MMC1.PDF.
[4] Lucas A, Chondrogiannis S. Smart grid energy storage controller for frequency regulation and peak shaving, using a vanadium redox flow battery. Int J Electr Power Energy Syst Sep. 2016;80:26–36. https://doi.org/10.1016/J.IJEPES.2016.01.025.
[5] Bhattacharjee A, Samanta H, Banerjee N, Saha H. Development and validation of a real time flow control integrated MPPT charger for solar PV applications of vanadium redox flow battery. Energ Conver Manage Sep. 2018;171:1449–62. https://doi.org/10.1016/J.ENCONMAN.2018.06.088.
[6] Sarkar T, Bhattacharjee A, Samanta H, Bhattacharya K, Saha H. Optimal design and implementation of solar PV-wind-biogas-VRFB storage integrated smart hybrid microgrid for ensuring zero loss of power supply probability. Energ Conver Manage Jul. 2019;191:102–18. https://doi.org/10.1016/J.ENCONMAN.2019.04.025.
[7] Hosseina M, Bathaee SMT. Optimal scheduling for distribution network with redox flow battery storage. Energ Conver Manage Aug. 2016;121:145–51. https://doi.org/10.1016/J.ENCONMAN.2016.05.001.
[8] ‘Ringo’, il primo esperimento a livello mondiale di un sistema di batterie. https://www.nidec-industrial.com/it/rte-nis-launches-ringo/; 2024 (accessed Oct. 14, 2023).
[9] All projects - Projects - Network development - TransnetBW. https://www.transnetbw.de/de/netzentwicklung/projekte/alle-projekte; 2024 (accessed Oct. 14, 2023).
[10] Dello M, Economico S. Piano Nazionale Integrato Per L’energia E Il Clima. 2024.
[11] Fast Reserve - Terna spa. https://www.terna.it/en/electric-system/pilot-projects-pursuant-arera-resolution-300-2017-reel/fast-reserve-pilot-project; 2024 (accessed Oct. 14, 2023).
[12] Alotto P, Guarnieri M, Moro F. Redox flow batteries for the storage of renewable energy: a review. Renew Sustain Energy Rev Jan. 2014;29:325–35. https://doi.org/10.1016/J.RSER.2013.08.001.
[13] Schmidt O, Melchior S, Hawkes A, Staffell I. Projecting the future Levelized cost of electricity storage technologies. Joule Jan. 2019;3(1):81–100. https://doi.org/10.1016/J.JOULE.2018.12.008.
[14] Baldinelli A, Barelli L, Bidini G, Discepoli G. Economics of innovative high capacity-to-power energy storage technologies pointing at 100% renewable microgrids. J Energy Storage Apr. 2020;28:101198. https://doi.org/10.1016/J.EST.2020.101198.
[15] Arbabzadeh M, Johnson JX, De Kleine R, Keoleian GA. Vanadium redox flow batteries to reach greenhouse gas emissions targets in an off-grid configuration. Appl Energy May 2015;146:397–408. https://doi.org/10.1016/J.APENERGY.2015.02.005.
[16] Guarnieri M, Mattavelli P, Petrone G, Spagnuolo G. Vanadium redox flow batteries: potentials and challenges of an emerging storage technology. IEEE Ind Electron Mag Dec. 2016;10(4):20–31. https://doi.org/10.1109/MIE.2016.2611760.
[17] Sánchez-Díez E, et al. Redox flow batteries: status and perspective towards sustainable stationary energy storage. J Power Sources Jan. 2021;481:228804. https://doi.org/10.1016/J.JPOWSOUR.2020.228804.
[18] Noack J, Roznyatovskaya N, Herr T, Fischer P. The chemistry of redox-flow batteries. Angew Chem Int Ed Aug. 2015;54(34):9776–809. https://doi.org/10.1002/ANIE.201410823.
[19] Vanitec. Global VRFB Installations Map. http://www.vanitec.org/; 2024 (accessed Feb. 20, 2023).
[20] Skyllas-Kazacos M. (Invited) Performance improvements and cost considerations of the vanadium redox flow battery. ECS Trans Apr. 2019;89(1):29. https://doi.org/10.1149/08901.0029ECST.
[21] U. S. D. of Energy. Grid Energy Storage. 2013.

[22] Noack J, Wietschel L, Roznyatovskaya N, Pinkwart K, Tübke J. Techno-economic modeling and analysis of redox flow battery systems. Energies Aug. 2016;9(8):627. https://doi.org/10.3390/EN9080627.
[23] Minke C, Turek T. Materials, system designs and modelling approaches in techno-economic assessment of all-vanadium redox flow batteries – a review. J Power Sources Feb. 2018;376:66–81. https://doi.org/10.1016/J.JPOWSOUR.2017.11.058.
[24] Li MJ, Zhao W, Chen X, Tao WQ. Economic analysis of a new class of vanadium redox-flow battery for medium- and large-scale energy storage in commercial applications with renewable energy. Appl Therm Eng Mar. 2017;114:802–14. https://doi.org/10.1016/J.APPLTHERMALENG.2016.11.156.
[25] Minke C, Kunz U, Turek T. Techno-economic assessment of novel vanadium redox flow batteries with large-area cells. J Power Sources Sep. 2017;361:105–14. https://doi.org/10.1016/J.JPOWSOUR.2017.06.066.
[26] Viswanathan V, et al. Cost and performance model for redox flow batteries. J Power Sources Feb. 2014;247:1040–51. https://doi.org/10.1016/J.JPOWSOUR.2012.12.023.
[27] Ha S, Gallagher KG. Estimating the system price of redox flow batteries for grid storage. J Power Sources Nov. 2015;296:122–32. https://doi.org/10.1016/J.JPOWSOUR.2015.07.004.
[28] Minke C, Dorantes Ledesma MA. Impact of cell design and maintenance strategy on life cycle costs of vanadium redox flow batteries. J Energy Storage Feb. 2019;21:571–80. https://doi.org/10.1016/J.EST.2018.12.019.
[29] Rodby KE, Carney TJ, Ashraf Gandomi Y, Barton JL, Darling RM, Brushett FR. Assessing the levelized cost of vanadium redox flow batteries with capacity fade and rebalancing. J Power Sources Jun. 2020;460:227958. https://doi.org/10.1016/J.JPOWSOUR.2020.227958.
[30] Yuan XZ, et al. A review of all-vanadium redox flow battery durability: degradation mechanisms and mitigation strategies. Int J Energy Res Oct. 2019;43(13):6599–638. https://doi.org/10.1002/ER.4607.
[31] Poli N, Bonaldo C, Trovo A, Guarnieri M. Optimal energy storage systems for long charge/discharge duration. ECS Meet Abstr Jul. 2022;MA2022-01(3):472. https://doi.org/10.1149/MA2022-013472MTGABS.
[32] Bonaldo C, Caporin M, Fontini F. The relationship between day-ahead and future prices in electricity markets: an empirical analysis on Italy, France, Germany, and Switzerland. Energy Econ Jun. 2022;110:105977. https://doi.org/10.1016/J.ENECO.2022.105977.
[33] Bonaldo C, Poli N. Vanadium redox flow batteries: characteristics and economic value. Lect Notes Networks Syst 2022;482 LNNS:1721–31. https://doi.org/10.1007/978-3-031-06825-6_166/COVER.
[34] Trovò A, Di Noto V, Mengou JE, Gamabaro C, Guarnieri M. Fast response of kW-class vanadium redox flow batteries. IEEE Trans Sustain Energy Oct. 2021;12(4):2413–22. https://doi.org/10.1109/TSTE.2021.3096573.
[35] Guarnieri M, Trovò A, D'Anzi A, Alotto P. Developing vanadium redox flow technology on a 9-kW 26-kWh industrial scale test facility: design review and early experiments. Appl Energy 2018;230(March):1425–34. https://doi.org/10.1016/j.apenergy.2018.09.021.
[36] Guarnieri M, Trovò A, Marini G, Sutto A, Alotto P. High current polarization tests on a 9 kW vanadium redox flow battery. J Power Sources 2019;431(May):239–49. https://doi.org/10.1016/j.jpowsour.2019.05.035.
[37] Kurilovich AA, Trovò A, Pugach M, Stevenson KJ, Guarnieri M. Prospect of modeling industrial scale flow batteries – from experimental data to accurate overpotential identification. Renew Sustain Energy Rev Oct. 2022;167:112559. https://doi.org/10.1016/J.RSER.2022.112559.
[38] Poli N, Schäffer M, Trovò A, Noack J, Guarnieri M, Fischer P. Novel electrolyte rebalancing method for vanadium redox flow batteries. Chem Eng J 2021;405(May 2020):126583. https://doi.org/10.1016/j.cej.2020.126583.
[39] Poli N, Trovò A, Fischer P, Noack J, Guarnieri M. Electrochemical rebalancing process for vanadium flow batteries: sizing and economic assessment. J Energy Storage Feb. 2023;58:106404. https://doi.org/10.1016/J.EST.2022.106404.
[40] Skyllas-Kazacos M. (Invited) Performance improvements and cost considerations of the vanadium redox flow battery. ECS Trans Apr. 2019;89(1):29. https://doi.org/10.1149/08901.0029ECST.
[41] What is the PUN | Enel Energia. https://www.enel.it/en/supporto/faq/cos-e-il-pun; 2024 (accessed Oct. 19, 2023).
[42] Gestore Mercati Elettrici (GME). No Title. https://www.mercatoelettrico.org/it/; 2024 (accessed Jul. 15, 2023).
[43] Bertolini M, D'Alpaos C, Moretto M. Do smart grids boost investments in domestic PV plants? Evidence from the Italian electricity market. Energy Apr. 2018;149:890–902. https://doi.org/10.1016/J.ENERGY.2018.02.038.
[44] No Title. Infront Analytics. https://www.infrontanalytics.com/; 2024 (accessed Oct. 23, 2023).
[45] Statista. Average market risk premium (MRP) for selected countries in Europe as of 2023. https://www.statista.com/statistics/664786/average-market-risk-premium-selected-countries-europe/; 2023.
[46] Shanghai Electric Group Co Ltd. Financial Time. 2023.
[47] Zakeri B, Syri S. Electrical energy storage systems: a comparative life cycle cost analysis. Renew Sustain Energy Rev Feb. 2015;42:569–96. https://doi.org/10.1016/J.RSER.2014.10.011.
[48] Charvát J, et al. Performance enhancement of vanadium redox flow battery by optimized electrode compression and operational conditions. J Energy Storage Aug. 2020;30:101468. https://doi.org/10.1016/J.EST.2020.101468.
[49] Mazúr P, et al. Performance evaluation of thermally treated graphite felt electrodes for vanadium redox flow battery and their four-point single cell characterization. J Power Sources Mar. 2018;380:105–14. https://doi.org/10.1016/J.JPOWSOUR.2018.01.079.
[50] Prieto-Díaz PA, Ibáñez SE, Vera M. Fluid dynamics of mixing in the tanks of small vanadium redox flow batteries: insights from order-of-magnitude estimates and transient two-dimensional simulations. Int J Heat Mass Transf Dec. 2023;216:124567. https://doi.org/10.1016/J.IJHEATMASSTRANSFER.2023.124567.
[51] Urban M. Cellcube in operation at Netz NÖ since 2011. 2021.
[52] Trovò A, Picano F, Guarnieri M. Comparison of energy losses in a 9 kW vanadium redox flow battery. J Power Sources 2019;440(August). https://doi.org/10.1016/j.jpowsour.2019.227144.
[53] Trovo A, Guarnieri M. Battery management system with testing protocols for kW-class vanadium redox flow batteries. In: Proc. - 2020 2nd IEEE Int. Conf Ind Electron Sustain Energy Syst IESES 2020; Sep. 2020. p. 33–8. https://doi.org/10.1109/IESES45645.2020.9210697.